

## Dielectric tunability of barium strontium titanate/silicone-rubber composite

This content has been downloaded from IOPscience. Please scroll down to see the full text.

1998 J. Phys.: Condens. Matter 10 2773

(<http://iopscience.iop.org/0953-8984/10/12/015>)

View [the table of contents for this issue](#), or go to the [journal homepage](#) for more

Download details:

IP Address: 140.113.38.11

This content was downloaded on 28/04/2014 at 11:57

Please note that [terms and conditions apply](#).

# Dielectric tunability of barium strontium titanate/silicone-rubber composite

J W Liou and B S Chiou

Department of Electronic Engineering and Institute of Electronics, National Chiao Tung University, Hsinchu 300, Taiwan, Republic of China

Received 2 June 1997, in final form 5 January 1998

**Abstract.** The dielectric tunability, which is defined as the percentage change of the permittivity under DC biasing, is over 30% for polycrystalline barium strontium titanate (BST) under a field of  $5000 \text{ V cm}^{-1}$  at around the Curie peak. Various volume fractions (18%, 40%, 52%, and 64%) of BST powder are mixed with silicone rubber to obtain a multi-phase dielectric composite. The effective permittivity of the composite follows the Maxwell-Garnett relation with a shape parameter of about 14 for volume fractions below 52%. The dielectric tunabilities at  $5000 \text{ V cm}^{-1}$  for the samples made with 52% and 64% powder are about 0.7% and 7.4%, respectively. The results are compared to the dielectric tunabilities obtained on the basis of series, parallel, and logarithmic models. It is suggested that the dielectric tunability is enhanced when a sample with a more continuous BST powder phase is obtained. An increase of the permittivity with a small DC field applied to the composite is attributed to the effect of polarization of the interface between the BST and silicone-rubber phases.

## 1. Introduction

Composite materials consisting of ferroelectric ceramics and polymers have aroused much interest because of their improved properties compared to those of the individual constituents [1–3]. In addition, their properties can be tuned according to requirements by changing the fractions of the constituents. The dielectric properties of some ferroelectrics are changed by DC biasing around the ferroelectric-to-paraelectric transition [4–5]. The coercive field for ferroelectric ceramics, such as barium titanate, is larger than  $10^6 \text{ V cm}^{-1}$  in the ferroelectric state. Hence, in applications using the DC biasing effect, it is preferable to suppress the Curie temperature ( $T_C$ ) of the ferroelectric material to below the application temperature so that the material can be employed in its paraelectric state. The phase angle of the signal is changed upon DC biasing in the application of barium strontium titanate (BST) in microwave phase shifters [6], and tunable capacitors [7]. Strontium suppresses the  $T_C$  of BST, so phase shifters and tunable capacitors can be utilized in the paraelectric state. Because of the brittle nature of ceramics, polymer is used to form a composite which is easy to incorporate into the electronic devices. Many studies have been done on the piezoelectric, dielectric, pyroelectric, elastic, and resistive properties of ceramic/polymer systems [2, 8–10]. Some model approaches [11–13] to the effective permittivity and piezoelectricity were also developed to explain the dielectric behaviour of the composite. However, few studies have been done on the effect of a DC field  $E$  on the dielectric properties of ceramic/polymer composite systems. Under DC biasing, the dielectric tunability  $D_t$  is defined as

$$D_t(E, T) = 1 - \frac{k(E, T)}{k(0, T)} \quad (1)$$

where the permittivity  $k(E, T)$  is a function of the field  $E$  and temperature  $T$ . The purpose of this study is to investigate the compositional dependence of the dielectric tunability on the dielectric properties of BST/silicone-rubber composite.

Silicones are based on polymers comprised of a backbone of silicon–oxygen–silicon atoms linked together. They are different from organic materials, which are mostly based on polymers composed of a backbone of carbon-to-carbon atoms linked together, as shown schematically in figure 1. The silicone bond linkage is similar to bond linkages found in other high-temperature-resistant materials such as quartz. Hence silicone rubber can withstand a higher temperature than natural rubber can. In addition, the high tear resistance and inherent release ability of silicone rubber make it well suited to the manufacture of intricate casting. In this study, various volume fractions of BST powder in silicone rubber are prepared to allow us to study the dielectric properties. The composition of the ceramic powder is  $\text{Ba}_{0.65}\text{Sr}_{0.35}\text{TiO}_3$  doped with 0.05 mol%  $\text{MnO}_2$  and 1.0 mol%  $\text{MgO}$ . The dopant  $\text{MnO}_2$  is used to trap the electrons to obtain low-loss dielectrics [14, 15] and the dopant  $\text{MgO}$  served as a grain growth inhibitor [16, 17]. The silicone-rubber compound used is a room temperature vulcanizing (RTV) liquid which cures, on the addition of a curing agent, to a resilient silicone rubber. For the comparison of the dielectric properties, pressed bulk and dispersive powder are heated according to a non-isothermal rate-controlled sintering profile [15–17] after the powder is calcined. The dielectric characteristics of both bulk BST and BST/silicone-rubber composite are investigated.

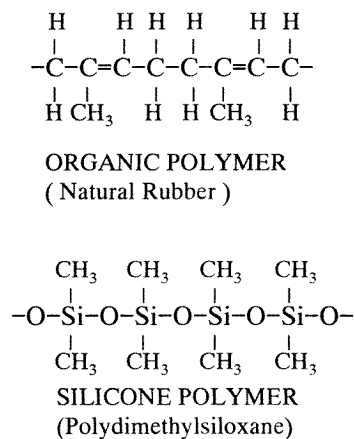


Figure 1. Schematic diagrams of the structures of organic rubber and silicone rubber.

## 2. Experimental procedures

Commercial powders of  $\text{BaCO}_3$ ,  $\text{SrCO}_3$ ,  $\text{TiO}_2$ ,  $\text{MnO}_2$ , and  $\text{MgO}$  (Merck & Company, Incorporated, Darmstadt, Germany) together with acetone were ball milled with alumina balls for 24 h. An excess of 1.0 mol% of  $\text{TiO}_2$  was added to obtain a  $\text{TiO}_2$ -rich liquid phase during sintering [15, 18]. After they were dried by means of IR illumination, the mixtures were calcined in an alumina crucible at 1100 °C for 2 h in air. Some of the powder was then mixed with a small amount of polyvinyl alcohol (PVA) binder and pressed to form disk-shaped samples at 180 MPa. The pressed bulk and the remaining powder were heated according to a controlled firing profile [15–17] after the binder was burned out at 400 °C for

2 h. This non-isothermal rate-controlled profile has an initial heating rate of  $80\text{ }^{\circ}\text{C min}^{-1}$  to  $1200\text{ }^{\circ}\text{C}$ , a temperature which was maintained for 6 min, and then heating up to  $1350\text{ }^{\circ}\text{C}$ , at the same heating rate, this latter temperature being maintained for 30 min. The samples were cooled down to room temperature at a rate of  $-5\text{ }^{\circ}\text{C min}^{-1}$ . Silicone rubber (RTV 630) obtained from General Electronic Company contains two components (RTV 630A and RTV 630B). Ten parts of component A and one part of component B were added together, as suggested by the vendor. The ceramic powder:silicone-rubber (A + B) weight ratios were chosen to be 1:1, 3:1, 5:1, and 8:1 corresponding to BST volume fractions of 18%, 40%, 52%, and 64%, respectively. The mixture was poured into an aluminium disk-shaped container and degassed in a vacuum chamber up to  $10^{-2}$  Torr. The curing process was carried out on a hot plate at  $100\text{ }^{\circ}\text{C}$  for 1 h.

A scanning electron microscope (SEM, Hitachi, S570, Japan) was employed to examine the surface morphology of the composite samples. The densities of the samples were measured by Archimedes' method. The specimens were 0.4 mm in thickness and 8.3 mm in diameter. In-Ga (40:60) alloy was rubbed on both surfaces to provide ohmic contacts. The permittivity of each sample was calculated from the capacitance measured with an HP4275A LCR meter (Hewlett-Packard Company). A 200V DC power supply was connected to the LCR meter as the external DC bias. The AC field applied was  $25\text{ V cm}^{-1}$ .

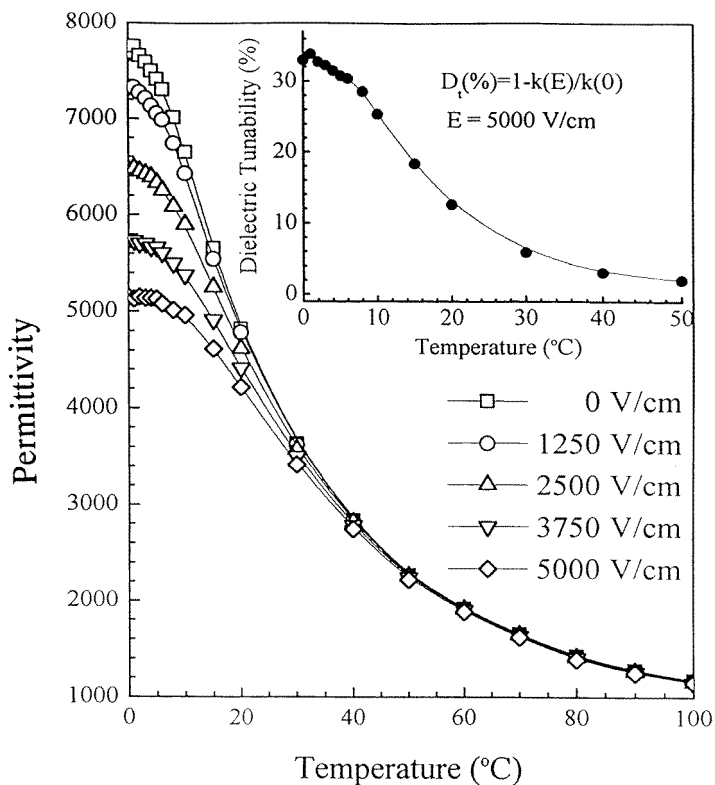


**Figure 2.** The temperature dependence of the permittivity at 1 MHz for bulk BST as a function of the DC field. The inset shows the temperature dependence of the dielectric tunability calculated at  $5000\text{ V cm}^{-1}$ .

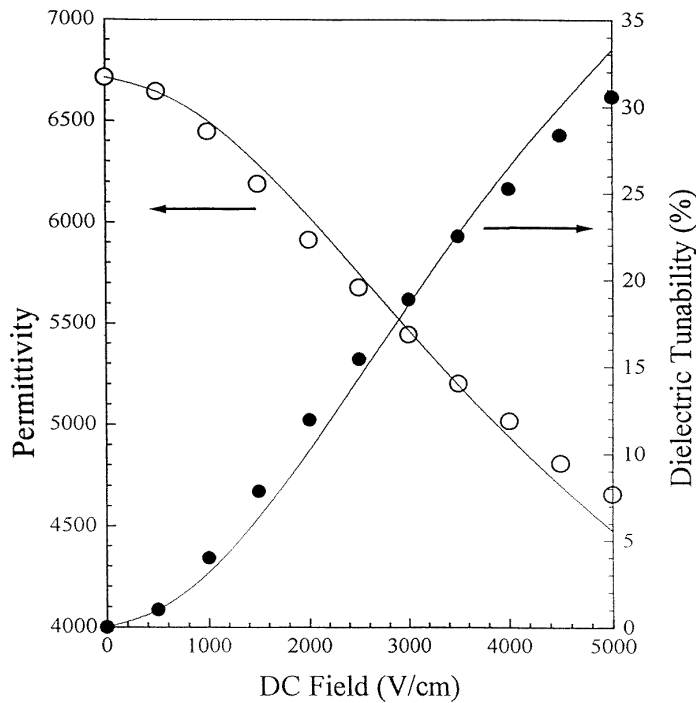


**Figure 3.** The DC-field dependence of the permittivity and dielectric tunability for bulk BST measured at 1 MHz and 10 °C. The solid lines are the curves fitted on the basis of equation (2).

### 3. Results and discussion

#### 3.1. The permittivity of BST and BST/silicone rubber

**3.1.1. Temperature dependence.** The temperature dependence of the permittivity at 1 MHz for bulk BST as a function of the DC field is shown in figure 2. The Curie temperature of this sample is 2 °C. The dielectric tunability of BST at 5000 V cm<sup>-1</sup>, calculated using equation (1), decreases as the temperature increases as shown in the inset of figure 2. The tunability drops to below 2.5% at temperatures above 50 °C. The DC-field dependence of the permittivity at constant temperature can be written in the form [4, 15, 17]

$$\frac{k(E)}{k(0)} = \frac{1}{[1 + a(k(0))^3 E^2]^{1/3}} \quad (2)$$

where  $a$  is a phenomenological coefficient. Equation (2) fits the measured data well as shown in figure 3. The dielectric tunability increases with the increase of the DC field. The 1 MHz permittivity and 5000 V cm<sup>-1</sup> tunability are 6654 and 30.6% at 10°C, respectively. The phenomenological coefficient  $a$ , obtained from figure 2, is  $3.13 \times 10^{19}$  cm<sup>2</sup> V<sup>-2</sup> which is comparable to values derived in previous work [4, 5, 15, 17].

The temperature dependence of the permittivity of composites with various BST fractions is shown in figure 4. A broadening of the dielectric peak is observed and the Curie temperatures of all of the samples in this study are ~2 °C, while in previous work by Muralidhar and Pillai [19], an absence of the Curie peak was reported for BaTiO<sub>3</sub>/PVDF composite. There are many possibilities for the cause of the suppression of the dielectric peak, such as: ultra-fine particles resulting in a locked tetragonal deformation by the surface

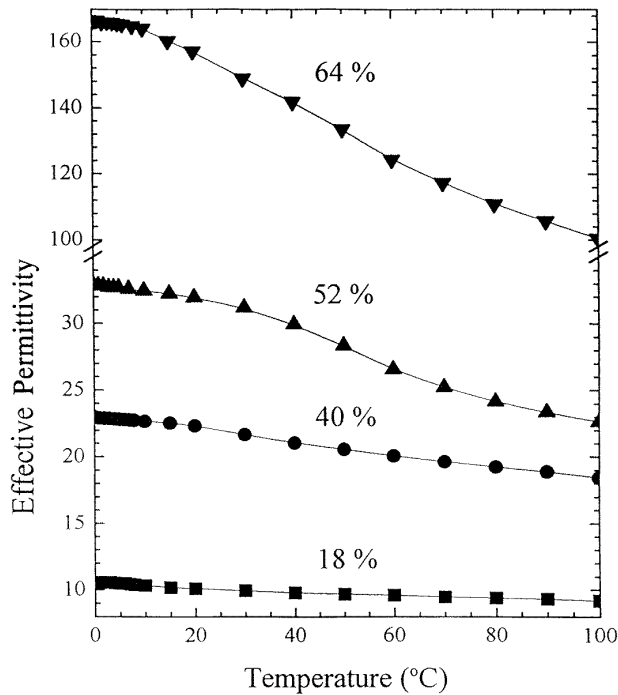
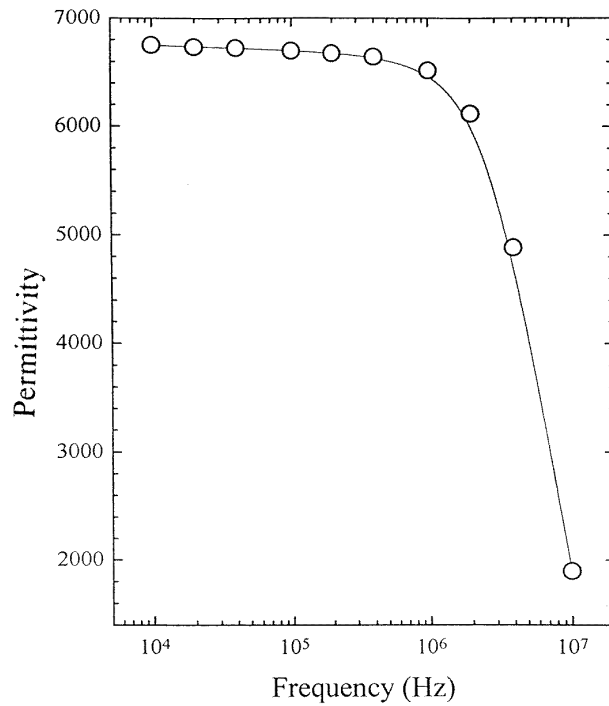


**Figure 4.** The temperature dependence of the permittivity at 1 MHz for composites with various BST volume fractions: 18%, 40%, 52%, and 64%.

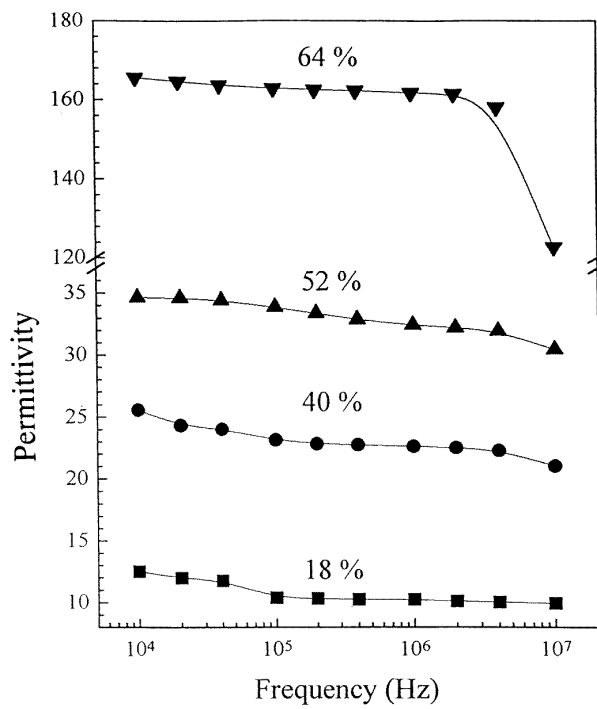
charge [20]; some chemical bonding between the ceramics and the polymer resulting in an off-valence of  $O^{2-}$  in BST [19]; and the diffuse phase in BST [21]. In this work, the particle size is about 5–10  $\mu\text{m}$ , while in Muralidhar and Pillai's work, ultra-fine particles of size less than 1  $\mu\text{m}$  were employed. If the stress exerted by the polymer suffices to deform the tetragonal structure to the cubic one of the powder, the Curie peak will disappear. In this study, the particle size is large enough to stand the stress without serious deformation of the structure, and it is believed that the BST is stable chemically during the curing process at 100  $^{\circ}\text{C}$ . Hence the Curie peak of BST/silicone-rubber composite is smeared instead of suppressed. The permittivity of the BST and silicone rubber are 6654 (10  $^{\circ}\text{C}$ ) and 3.2 [22]. Because the BST particles, with high permittivity, were dispersed in a matrix with low permittivity, the temperature dependence of the permittivity was broadened.

**3.1.2. Frequency dependence.** The frequency dependences of the permittivity of BST bulk and the composite with various volume fractions at 10  $^{\circ}\text{C}$  are shown in figures 5(a) and 5(b), respectively. The rapid decline of the permittivity for BST bulk above 1 MHz is due to the dipolar relaxation in the ceramics [23]. As the volume fraction of BST decreases, the variation of the permittivity with the frequency becomes less, as shown in figure 5(b). Another cause of this behaviour is the dispersion of BST particles in silicone rubber.

**3.1.3. Surface morphology.** In the composite, the BST phase is dispersed in a continuous silicone rubber matrix as shown in figures 6(a) and 6(b). As seen from the SEM pictures of composites with 52% and 64% BST, there are pores on the surface of these composites.



(a)



(b)

**Figure 5.** The frequency dependence of the permittivity at 10 °C (a) for BST bulk and (b) for composites with various BST volume fractions.

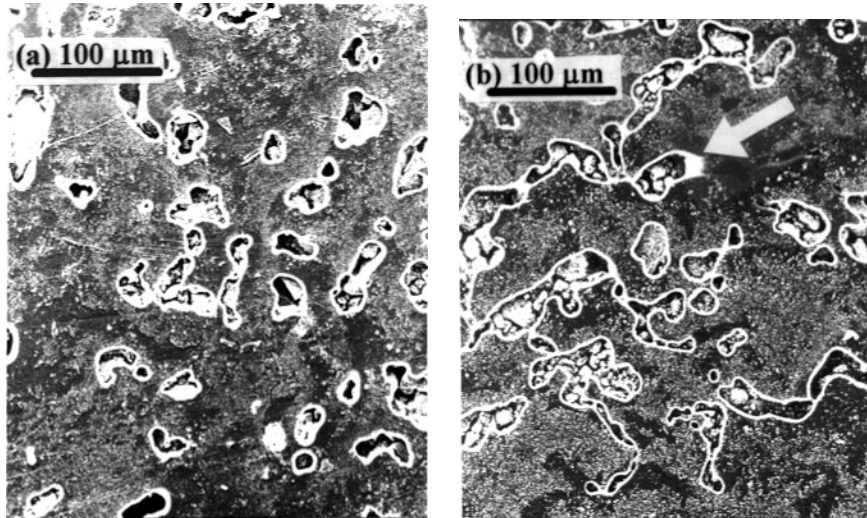


**Figure 6.** The surface morphology of the composite with BST volume fractions of (a) 52% and (b) 64%. The arrow points to the open pore which is due to the BST powders falling off the surface.

The dimensions of these pores are several tens of  $\mu\text{m}$ . The area fractions of these open pores were estimated to be about 18% and 24% for composites with 52% and 64% BST. As the volume fraction of BST increases, the amount of BST particles exposed on the surface of the composite increases and some of the BST powder on the composite surface fell off when the cured composite was removed from the disk-shaped container. Few open pores were observed on the samples with 18% and 40% BST. The theoretical densities  $D_{th}$  of composites are calculated on the basis of the densities of bulk BST ( $5.71 \text{ g cm}^{-3}$ ) and silicone rubber ( $1.28 \text{ g cm}^{-3}$ ). The measured densities of the composites with 52% and 64% BST are 95.7% of  $D_{th}$  and 93.3% of  $D_{th}$ , respectively. It is noted that the porosities of these two samples (4.3% and 6.7%) are much lower than the area fractions of the open pores (18% and 24%).

**3.1.4. The mixture model for multi-phase dielectrics.** Several macroscopic mixture models have been proposed [11–13] for calculating the effective permittivity of multi-phase dielectric systems. In this study, the composite consists of three phases, BST powder, silicone rubber and pores. Because the permittivities of silicone rubber (3.2) and the pores (1) are very small compared to that of BST (6654), it is assumed that the matrix is made of silicone rubber with pores. In this matrix, the high-permittivity BST phase was dispersed. The permittivity of the matrix with pores in it ranges between 1.84 (calculated on the basis of a dielectric series model) and 2.38 (calculated on the basis of a dielectric parallel model). These values are 0.028% to 0.036% of the permittivity of BST. The composite is then treated as a two-phase dielectric consisting of a low- $k$  matrix ( $k \sim 2.11$ ) dispersed with a high- $k$  dielectric ( $k \sim 6654$ ). Figure 7 exhibits the measured permittivity of the composite and the theoretical predictions made on the basis of the dielectric parallel model, the series model, the logarithmic model, Niesel's model, and the Maxwell-Garnett (M-G) model [8]. Among these models, the M-G model fits the measured permittivity for the BST volume up to 52%. The M-G model calculates the field and potential distribution in a binary system



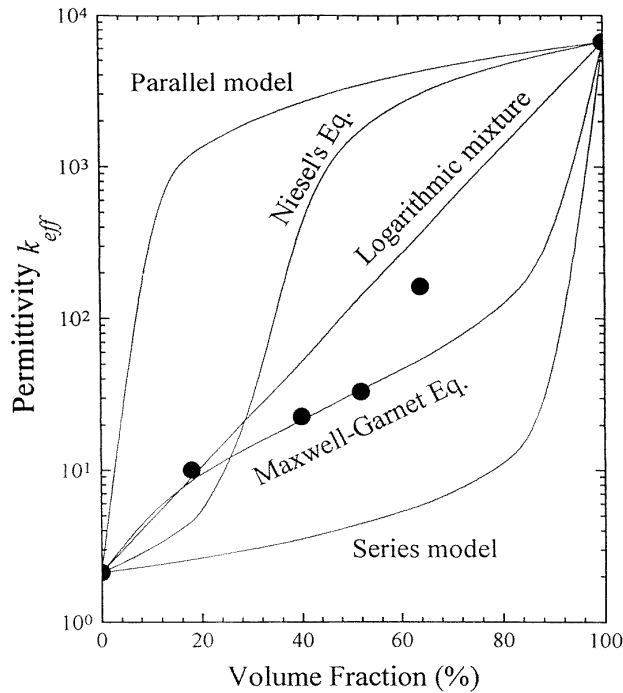


**Figure 7.** The effective permittivity  $k_{eff}$  of composites at 10 °C and the predictions made on the basis of the dielectric parallel model, the series model, the logarithmic mixture model, Niesel's model, and the Maxwell-Garnett model.

composed of ellipsoidal particles with permittivity  $k_1$  as an inclusion in a periodic-element continuous medium with permittivity  $k_2$ . The whole system is assumed to be constructed of numerous units of this kind of periodic element. This physical picture is similar to the structure of the BST/silicone-rubber composite. The effective permittivity  $k_{eff}$ , obtained on the basis of the M-G model, is

$$k_{eff} = k_2 \left[ 1 + \frac{nv_1(k_1 - k_2)}{nk_2 + (k_1 - k_2)(1 - v_1)} \right] \quad (3)$$

where  $v_1$  and  $v_2$  are the volume fractions of the two phases with the corresponding permittivities  $k_1$  and  $k_2$ , respectively, and  $n$  is the parameter attributed to the shape of the ellipsoidal particles.

The shape parameter  $n$  in this study is 14.0, which demands an ellipsoid axis ratio of  $\sim 4.2$ , and the long ellipsoids arranged perpendicular to the field direction. The calculation of the shape parameter from the axis ratio is given in the appendix of this article. Since BST powders were mixed thoroughly with silicone rubber before curing, a homogeneous mixture with uniformly distributed BST particles was expected, and a shape parameter of 3 and an axis ratio of 1 were anticipated. It is believed that there are two possible causes of the high values of the shape parameter: the clustering of BST particles and the exposure of particles on the surface as shown in figure 6. For samples with high BST contents ( $>52\%$  in this study), some BST powders contact and form continuous chains which enhance the temperature sensitivity and the frequency response as shown in figures 4 and 5. Also, the composite surface with open pores covered conformably by the In-Ga electrode results in an

increase of the effective electrode area and a decrease of the effective dielectric thickness. This raises the permittivity. In the work of Tao *et al* [24], a first-principles Fourier approach was used to calculate the effective permittivity of periodic composite. The permittivities that they obtained are larger than those predicted using the M-G equation when the volume fraction of high- $k$  phase exceeds 50%. Sareni *et al* [13] took the clustering effect into consideration and found that beyond a packing threshold of 52.3 vol%, the particles were no longer isolated, and the  $k_{eff}$ -values were higher than those predicted using the M-G model. In this study, a deviation of the permittivity from the M-G prediction is found for the sample with 64% BST as seen in figure 7. As the volume fraction of high- $k$  particles increases, the separation between particles decreases, and particles are exposed to the local fields induced by each other.

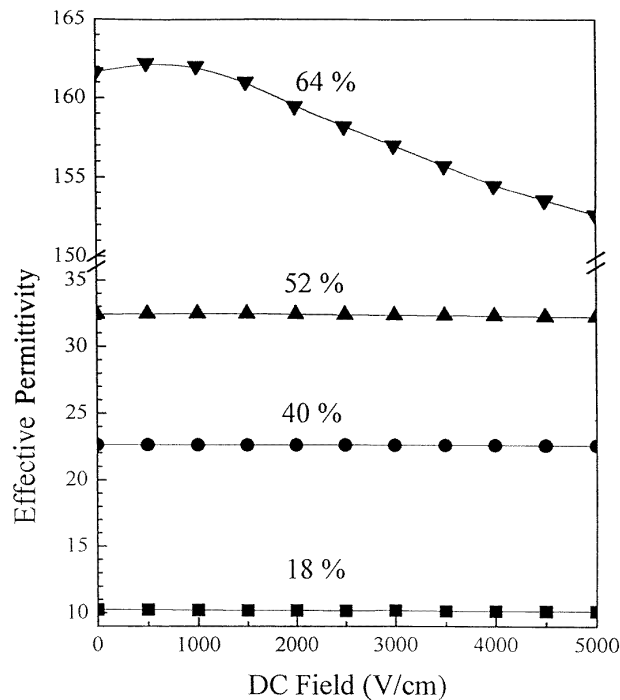


**Figure 8.** The DC-field dependence of the permittivity at 10 °C for composites with various BST volume fractions: 18%, 40%, 52%, and 64%.

### 3.2. Dielectric tunability of BST/silicone rubber

**3.2.1. DC-field dependence.** The DC-field dependences of the permittivity at 10 and 1 MHz for composites with various powder fractions are shown in figure 8. The dielectric tunability for the sample with a 64% powder fraction calculated using equation (1) is about 7.4% at a DC field of 5000 V cm<sup>-1</sup>. This dielectric tunability is much higher than those for the samples with 52% and 40% powder fractions, of about 0.7% and 0.15%, respectively. As the DC field is applied to the composite, only the field exerted on the BST phase contributes to the dielectric tunability measured. Therefore, the field distribution in the composite is crucial to the dielectric tunability. The simple parallel and series models represent two

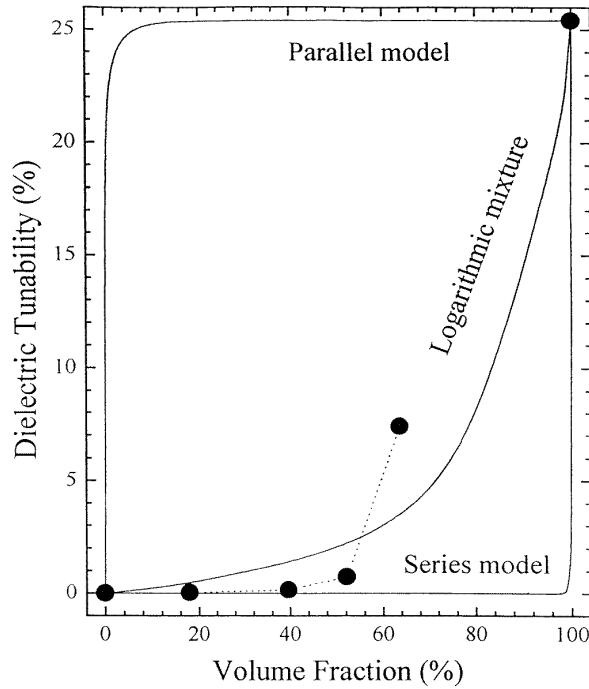


**Figure 9.** The dielectric tunabilities of composites and the predictions made on the basis of three dielectric connective models (solid lines).

extreme cases that can help us to understand the relation between the field distribution and the dielectric tunability. In the parallel model, the internal fields  $E_1$  in phase 1 and  $E_2$  in phase 2 are equal to the applied field  $E$ . This case is similar to that of a composite with a continuous phase of BST powder in it. Assume that  $k_2$ , the permittivity of silicone rubber, is constant for varying DC field. Then the effective tunability of the composite can be obtained using equation (1):

$$D_t(E) = \frac{v_1 k_1 D_{t1}(E_1)}{v_1 k_1 + v_2 k_2} \quad (4)$$

where  $D_{t1}(E_1)$  is the dielectric tunability of the BST and equals  $D_{t1}(E)$  in the parallel model. Equation (4) gives the upper limit of the dielectric tunability. In the series model, the internal field  $E_1$  is a part of the total applied field  $E (=v_1 E_1 + v_2 E_2)$ . From the boundary condition at the interface of these two phases (i.e.,  $k_1 E_1 = k_2 E_2$ ), one gets

$$E_1 = \frac{k_2 E}{v_1 k_2 + v_2 k_1}. \quad (5)$$

This is the case for BST powders individually embedded in the composite. Thus  $D_{t1}(E_1)$  is no longer equal to  $D_{t1}(E)$  for the series model. The dielectric tunability of BST bulk is approximately proportional to the applied field, as revealed in figure 3. That is,

$$D_{t1}(E_1) \approx \frac{E_1}{E} D_{t1}(E). \quad (6)$$

From equations (1), (5), and (6), the tunability for the series model is obtained:

$$D_t(E) = \frac{v_1 k_2^2 D_{t1}(E)}{(v_1 k_2 + v_2 k_1)^2 - v_2 k_1 k_2 D_{t1}(E)}. \quad (7)$$

Equation (7) gives the lower limit of the dielectric tunability. As for a logarithmic mixture, an assumption is made regarding the internal field in phase 1:

$$E_1 = \frac{\log k_2}{v_1 \log k_2 + v_2 \log k_1} E. \quad (8)$$

With equations (1) and (8) and the logarithmic model, the dielectric tunability for a logarithmic mixture can be obtained:

$$D_t(E) = 1 - \left[ 1 - \frac{D_{t1}(E) \log k_2}{v_1 \log k_2 + v_2 \log k_1} \right]^{v_1}. \quad (9)$$

The measured dielectric tunabilities and theoretical predictions made on the basis of the above three models are shown in figure 9. A nearly rectangular plot bounded by the parallel and series model predictions is observed for the  $D_t$  versus volume fraction curves. This is because the dielectric tunability in a composite is determined by how much the field concentrates on the BST phase. Therefore, the connectivity of the dielectrically tunable phase in the composite is crucial to the tunability. An abrupt rise in dielectric tunability is observed for the sample with 64% BST. This suggests the formation of continuous chains of BST as mentioned previously.

**3.2.2. Frequency dependence.** The permittivity as a function of the DC field at various frequencies for BST bulk and the composite with 64% powder are shown in figures 10(a) and 10(b), respectively. The DC field reduces the permittivities for the frequency range from 10 kHz to 4 MHz. But under small fields ( $E \leq 1000 \text{ V cm}^{-1}$ ), a small increase of permittivity for the composite is observed, and this increase becomes smaller at higher frequencies. No such behaviour is observed for bulk BST as shown in figure 10(a). The internal field  $E_1$  in the BST phase is very small compared to  $E_2$  due to the large permittivity ratio of phase 1 to phase 2 as inferred from equation (5). The internal field  $E_1$  would not affect the Curie peak ( $T_C$ ) of the BST phase since no shift in  $T_C$  is observed for a field strength as high as  $5000 \text{ V cm}^{-1}$ , as shown in figure 2. Hence, the increase in the permittivity is not caused by the shift in  $T_C$ . However, if some charges are induced at the interface between the BST powders and the polymers by the DC field, additional interfacial polarization is included in the total polarization measured. Therefore, in this two-phase system, the interfacial polarization is argued to be responsible for the increase of the permittivity at small DC biasing field, and the permittivity is raised, as seen in figure 10(b), for  $E \leq 1000 \text{ V cm}^{-1}$ . At high frequencies, the interfacial polarization lags behind the charging field, and the increase in  $k$  at low  $E$  is not appreciable, as observed in the 4 MHz plot in figure 10(b).

#### 4. Summary

(1) The dielectric characteristics of BST/silicone rubber composites with powder volume fractions of 18%, 40%, 52%, and 64% are investigated. The Maxwell-Garnett model predicts the permittivity up to 52%. A shape parameter  $n$  of about 14 is obtained. The clustering of BST powder and the surface effect lead to this high  $n$ -value.

(2) The effective permittivity for the composite with 64% BST is 161.6 which is larger than the prediction of the M-G model. This is attributed to the field interaction among the BST powders as the volume fraction exceeds a packing threshold.

(3) The dielectric tunability for the composite with 64% BST is 7.4% which is much larger than that of the composite with less BST powder. Some continuous region of high-

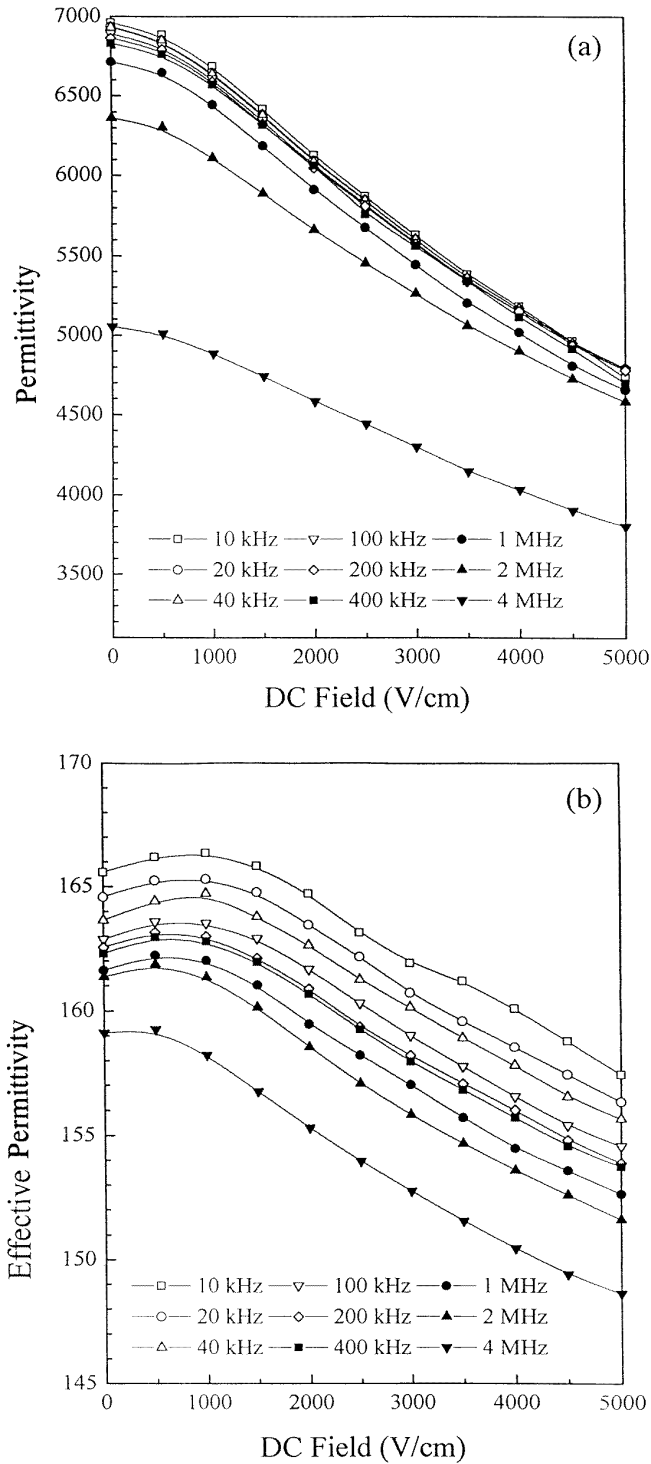


**Figure 10.** The permittivity as a function of the DC field at various frequencies for (a) the bulk sample of BST and (b) the composite with 64% BST powder. The temperature is 10 °C.

permittivity phase is believed to exist in the composite with the high powder volume fraction. Hence the dielectric tunability is effectively enhanced.

(4) The tunability versus volume fraction plot suggests that the effective dielectric tunability strongly depends on the field distribution in the composite.

(5) Under DC biasing, the effect of interfacial polarization which results in an increase of the permittivity is observed in the two-phase system with a large difference in permittivity.

### Acknowledgments

This work was supported by the Chung-Shan Institute of Science and Technology and partly supported by the National Science Council of Taiwan, Republic of China (contract Nos CS 85-0210-D-009-009 and NSC 86-2623-D-009-002).

### Appendix

The shape parameter of the ellipsoid is the inverse of the depolarization factor in the field direction; that is,

$$\frac{1}{n} = \frac{a^2 c}{2} \int_0^\infty \frac{du}{(c^2 + u)^{3/2} (a^2 + u)} \quad (\text{A1})$$

where  $a$  and  $c$  are the axis lengths of the ellipsoid perpendicular and parallel to the applied field. The axis ratios (from 0.1 to 4.5) versus the shape parameters are plotted in figure A1.

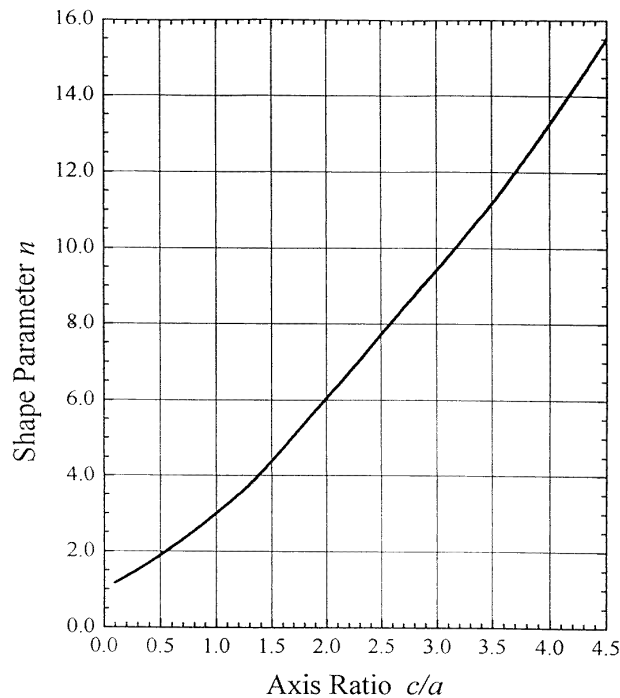


**Figure A1.** The axis ratio  $c/a$  of the ellipsoid versus the shape parameter  $n$  calculated from equation (A1).

An axis ratio of 1 indicates a spherical particle and corresponds to an  $n$ -value of 3. Thus the Maxwell-Garnett equation reduces to the famous Clausius–Mossotti form:

$$\frac{k_{eff} - k_2}{k_{eff} + 2k_2} = v_1 \frac{k_1 - k_2}{k_1 + 2k_2}. \quad (\text{A2})$$

## References

- [1] Newnham R E 1986 *Ferroelectrics* **68** 1
- [2] Muralidhar C and Pillai P K C 1987 *J. Mater. Sci. Lett.* **6** 1243
- [3] Pillai P K C, Lew J J, Gavrielides A and Clayton C M 1991 *J. Mater. Sci.* **26** 2671
- [4] Johnson K M 1962 *J. Appl. Phys.* **33** 2826
- [5] Qutzourhit A, Trefny U, Kito T and Yarar B 1995 *J. Mater. Res.* **10** 1411
- [6] Selmi F, Hughes R, Varadan V K and Varadan V V 1993 *Proc. SPIE* **1916** 180
- [7] Galt D, Price J C, Beall J A and Ono R H 1993 *Appl. Phys. Lett.* **63** 3078
- [8] Yamada T, Ueda T and Kitayama T 1982 *J. Appl. Phys.* **53** 4328
- [9] Broadhurst M G and Davis G T 1984 *Ferroelectrics* **60** 3
- [10] Sekar R, Tripathi A K and Pillai P K C 1989 *Mater. Sci. Eng. B* **5** 33
- [11] Tinga W R, Voss W A G and Blossey D F 1973 *J. Appl. Phys.* **44** 3897
- [12] Shen L C, Liu C, Korringa J and Dunn K J 1990 *J. Appl. Phys.* **67** 7071
- [13] Sareni B, Krähenbühl L, Beroual A and Brosseau C 1996 *J. Appl. Phys.* **80** 1688
- [14] Batllo F, Duverger E, Jules J C, Niepce J C, Jannot B and Maglione M 1990 *Ferroelectrics* **109** 113
- [15] Liou J W and Chiou B S 1998 *J. Am. Ceram. Soc.* at press
- [16] Chiou B S, Koh C M and Duh J G 1987 *J. Mater. Sci.* **22** 3893
- [17] Liou J W and Chiou B S 1997 *J. Appl. Phys.* **36** 4359
- [18] Anderson H U 1973 *J. Am. Ceram. Soc.* **56** 605
- [19] Muralidhar C and Pillai P K C 1987 *J. Mater. Sci. Lett.* **6** 346
- [20] Lee B W and Auh K H 1995 *J. Mater. Res.* **10** 1418
- [21] Tiwari V S, Singh N and Pandey D 1995 *J. Phys.: Condens. Matter* **7** 1441
- [22] Product data of RTV 630, General Electronic Company.
- [23] Kersten O, Rost A and Schmidt G 1988 *Ferroelectrics* **81** 31
- [24] Tao R, Chen Z and Sheng P 1990 *Phys. Rev. B* **41** 2417